

RSC Advances



This is an *Accepted Manuscript*, which has been through the Royal Society of Chemistry peer review process and has been accepted for publication.

Accepted Manuscripts are published online shortly after acceptance, before technical editing, formatting and proof reading. Using this free service, authors can make their results available to the community, in citable form, before we publish the edited article. This *Accepted Manuscript* will be replaced by the edited, formatted and paginated article as soon as this is available.

You can find more information about *Accepted Manuscripts* in the [Information for Authors](#).

Please note that technical editing may introduce minor changes to the text and/or graphics, which may alter content. The journal's standard [Terms & Conditions](#) and the [Ethical guidelines](#) still apply. In no event shall the Royal Society of Chemistry be held responsible for any errors or omissions in this *Accepted Manuscript* or any consequences arising from the use of any information it contains.



Injectable supramolecular hydrogels fabricated from PEGylated doxorubicin prodrug and α -cyclodextrin for pH-triggered drug delivery

Received 00th January 20xx,
Accepted 00th January 20xx

Fei Li,^a Jinlin He,^a Mingzu Zhang,^a Kam Chiu Tam,^b Peihong Ni^{a*}

DOI: 10.1039/x0xx00000x

www.rsc.org/

Supramolecular hydrogels, which are held together by noncovalent bonds and show responses to external stimuli, are of great interest in therapeutic delivery and tissue engineering as the injectable depot systems. To obtain a supramolecular hydrogel with multifunctions, such as low cytotoxicity, injectability and stimuli-triggered drug release, we herein report on the synthesis and characterization of a supramolecular hydrogel, which was formed by host-guest interaction between α -cyclodextrin (α -CD) and a PEGylated doxorubicin prodrug linked with an acid-cleavable hydrazone group (mPEG-Hyd-DOX). The polymeric prodrug displayed lower cytotoxicity than the free DOX. The host-guest interaction was demonstrated by X-ray diffraction (XRD) analysis. The structures and morphologies of the supramolecular hydrogels were systematically investigated by differential scanning calorimetry (DSC), scanning electron microscopy (SEM) and thermogravimetric analysis (TGA). The sol-gel transition process was monitored by dynamic and steady rheological analysis. The hydrogels could be degraded in the acidic environment of tumor cells and achieved the controlled delivery of DOX. The results of pH-responsive property, *in vitro* cytotoxicity and drug release revealed that the supramolecular hydrogels can be used as a potential injectable matrix for the encapsulation and controlled release of hydrophobic anticancer drugs. This study provides an alternative for the construction of dual- or multi-drug delivery systems.

Introduction

Supramolecular hydrogels are a class of water-swollen polymeric networks with distinct three-dimensional structures and they are usually fabricated by crosslinking with supramolecular interactions.^{1,2} The concepts and achievements of supramolecular hydrogels have drawn immense attentions in recent years and these materials have emerged as promising biomaterials because of their excellent biocompatibility, permeability, and ability to load bioactive agents, such as drugs,³⁻⁶ proteins,^{7,8} genes⁹ and even living cells.¹⁰ The soft and pliable properties of hydrogels could also minimize the mechanical irritation and damage to the surrounding tissue, typically reducing protein adsorption and thus inflammatory response in tissue engineering.^{11,12} It is worth noting that supramolecular hydrogels, unlike conventional chemical hydrogels, are based on relatively weak non-covalent interactions, such as hydrophobic

interaction,^{13,14} inclusion complexation,¹⁵⁻¹⁸ ionic interaction,¹⁹⁻²¹ metal-ligand coordination,²² biomimetic interaction,^{23,24} and so on. Among them, the inclusion complexation involving interactions of cyclodextrins (CDs) and various guest molecules have been employed in supramolecular chemistry for many years, and have progressively sparked polymer scientists' attention in this field.^{2,25-28} For example, Allcock *et al.* reported an injectable supramolecular hydrogel formed between mPEG modified biodegradable polyphosphazenes and α -CD, and used for protein delivery.²⁹ Harada *et al.* prepared a transparent supramolecular hydrogel that was quickly formed upon mixing β -CD-modified poly(acrylic acid) (PAA) with ferrocene-modified PAA, and it can be used as the redox-responsive self-healing material.³⁰ Jiang *et al.* obtained a photoreversible pseudopolyrotaxane hydrogel by simply utilizing the competition of three host-guest interactions among *trans*-Azo-C1-N⁺/ α -CD, PEG/ α -CD, and *cis*-Azo-C1-N⁺/ α -CD.³¹ These supramolecular hydrogels are easier to be formed and modulated under mild conditions, and they can carry various drugs for applications in the controlled release and tissue engineering.

Over the past years, rapid growth of drug delivery systems have been achieved, such as nanoparticles,³² polymeric micelles,³³⁻³⁵ hyperbranched polymers,³⁶ dendrimers,^{37,38} liposomes,³⁹ polymersomes⁴⁰ and polymeric prodrugs.^{41,42} In particular, polymeric prodrugs have been considered as one of the most promising manners to improve the efficacy of drug

^a College of Chemistry, Chemical Engineering and Materials Science, Suzhou Key Laboratory of Macromolecular Design and Precision Synthesis, Jiangsu Key Laboratory of Advanced Functional Polymer Design and Application, Soochow University, Suzhou 215123, P. R. China. Tel: +86 512 65882047; E-mail: phni@suda.edu.cn.

^b Department of Chemical Engineering, University of Waterloo, 200 University Avenue West, Waterloo, Ontario, N2L 3G1, Canada.

Electronic Supplementary Information (ESI) available: [details of any supplementary information available should be included here]. See DOI: 10.1039/x0xx00000x

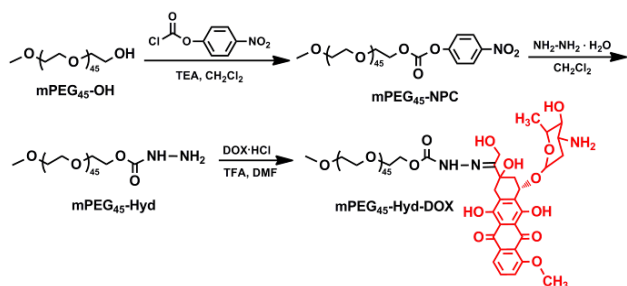
treatment. Typically, the drug molecules are conjugated to the hydrophilic polymers such as poly(ethylene glycol), acrylic polymers, or polysaccharides,^{41,43,44} and generally possess some advantages including the increased water solubility, lower systemic toxicity, and prolonged circulation time.⁴⁵ To further strengthen the therapeutic efficacies and pharmaceutical properties of polymeric prodrugs, much more efforts have been done to the hydrogel matrix for the encapsulation and delivery of drugs. For instance, Zhang *et al.* prepared a hydrogel formed by PEGylated indomethacin with α -CD for the controlled and sustained drug release.⁴⁶ Shi *et al.* reported a multifunctional supramolecular hydrogel based on host-guest inclusion for the codelivery of two different anticancer drugs.⁴⁷

Doxorubicin (DOX) has been demonstrated to possess broad spectrum antitumor activity against various cancers including breast,⁴⁸ ovarian⁴⁹ and gastric cancers,⁵⁰ as well as the acute lymphoblastic-leukemia, alone or in combination with other agents.⁵¹ To date, many kinds of DOX-based polymeric prodrug have been proposed,^{41,45,52-55} however, the supramolecular hydrogels constructed from these prodrugs are rarely investigated. Herein, considering the acidic environment in tumor tissues,^{56,57} we first synthesized a polymeric prodrug composed of mPEG and DOX linked with acid-labile hydrazine group (designated as mPEG-Hyd-DOX), as shown in Scheme 1. Subsequently, a series of injectable drug-encapsulated supromolecular hydrogels were prepared *via* the inclusion complexation interaction of mPEG-Hyd-DOX and α -CD. The sol-gel transition, mechanical strength and shear-thinning behavior were monitored by dynamic and steady rheological analysis. In addition, the *in vitro* cytotoxicity and pH-responsive drug release were also studied for this prodrug loaded in the supramolecular hydrogel matrix.

Experimental

Materials

Poly(ethylene glycol) monomethyl ether (mPEG₄₅-OH, $\overline{M}_n \approx 2000$ g mol⁻¹, PDI = 1.06, Sigma-Aldrich), 4-nitrophenyl chloroformate (NPC, 97%, Alfa Aesar), doxorubicin hydrochloride (DOX-HCl, 99%, Beijing Zhongshuo Pharmaceutical Technology Development), hydrazine monohydrate (85%, Sinopharm Chemical Reagent), trifluoroacetic acid (TFA, 99%, Acros) and α -cyclodextrin (α -CD,



Scheme 1. Synthesis of mPEG₄₅-Hyd-DOX prodrug.

G.R., TCI) were used as received. Triethylamine (TEA, A.R.) and *N,N*-dimethylformamide (DMF, A.R.) were purchased from Sinopharm Chemical Reagent, separately dried over anhydrous MgSO₄ for 24 h, and then distilled under reduced pressure before use. Toluene (A.R.) and dichloromethane (CH₂Cl₂, A.F.) were obtained from Sinopharm Chemical Reagent, and individually dried over CaH₂ for 24 h at room temperature, then followed by distillation just before use. Milli-Q water (18.2 M Ω cm⁻¹) was generated using a water purification system (Simplicity UV, Millipore). All the other reagents and solvents were of analytical grade, obtained from Sinopharm Chemical Reagent and used as received unless otherwise mentioned. All cell culture related reagents were purchased from Invitrogen/Life Technologies.

Instruments

Nuclear magnetic resonance (NMR) spectra were performed on a 400 MHz Bruker NMR spectrometer (INOVA-400, Varian) at 25 °C with CDCl₃ or DMSO-*d*₆ as the solvent and TMS as the internal reference. FT-IR spectra were recorded on a Nicolet 6700 spectrometer using the KBr disk method. The interior structures of the hydrogels were observed by scanning electron microscopy (SEM) using a Quanta 200 FEG electron microscope operating at 15 kV. The mixture of prodrug solution and α -CD solution was added on the surface of a silicon SEM specimen holder, let stand for 5 min, quickly frozen in liquid nitrogen and further freeze-dried in a freeze drier at -40 °C for 3 days until all the solvent was sublimed. The freeze-dried hydrogel was sputter coated with gold before observation. XRD patterns were recorded on a Rigaku D/max 2500 X-ray powder diffractometer using Cu K α (1.54 Å) radiation (50 kV, 250 mA). All samples were scanned from 2 θ = 5° to 45° at a speed of 5° min⁻¹. DSC was carried out on a DSC TA-60WS thermal analysis system (Shimadzu, Japan). Samples were first heated from -40 °C to 100 °C at a heating rate of 10 °C min⁻¹ under a nitrogen atmosphere, followed by cooling to -40 °C after stopping at 100 °C for 3 min, and finally heating to 180 °C at 10 °C min⁻¹. Thermogravimetric analysis (TGA) was examined on a Pyris 1 TGA (Perkin Elmer, USA) with a heating rate of 20 °C min⁻¹ from 80 to 500 °C under a nitrogen atmosphere. HPLC (Agilent 1260 infinity series) uses a C18 reversed phase column (4.6 × 150 mm, 5 μ m) at 30 °C and a UV detector conducted at 254 nm. The mobile phase consisted of acetonitrile (HPLC grade, Sinopharm Chemical Reagent)-water (Milli-Q water) (v/v, 50/50) with a flow rate of 1.0 mL min⁻¹. The data were analyzed by Chem-Station software. The fluorescence spectra were recorded on a spectrofluorometer (FLS920, Edinburgh). The excitation was carried out at 480 nm and the emission spectra were recorded at 560 nm with the slit width for both excitation and emission set at 1 nm.

Synthesis of mPEG₄₅-Hyd-DOX prodrug

Synthesis of mPEG₄₅-NPC. The mPEG₄₅-OH (2.0 g, 1.0 mmol) was dried by azeotropic distillation with toluene just before use. Under a dry nitrogen atmosphere, the purified mPEG₄₅-OH was dissolved in 10 mL of anhydrous CH₂Cl₂, and the solution was added dropwise

over 30 min into a flask containing NPC (0.8 g, 4.0 mmol) and anhydrous CH_2Cl_2 (50 mL) at 0 °C, which was then vigorously stirred at 25 °C for 24 h. The mixture was diluted with 60 mL of CH_2Cl_2 and washed three times with 10 mL of 5% NH_4Cl solution. The combined organic phase was dried over anhydrous Na_2SO_4 for 4 h, concentrated and precipitated into cold diethyl ether twice. The product was collected by filtration and dried under vacuum for 24 h to give mPEG₄₅-NPC with a yield of 90%. ^1H NMR (400 MHz, CDCl_3 , 25 °C, ppm, Fig. S1(B)†): δ 3.38-3.40 (peak a, 3H), δ 3.44-3.84 (peak b, 180 H), δ 4.43-4.48 (peak c, 2H), δ 7.38-7.43 (peak d, 2H), δ 8.27-8.32 (peak e, 2H).

Synthesis of mPEG₄₅-Hyd. The hydrazine monohydrate (0.294 g, 5.0 mmol) was dissolved in 50 mL of anhydrous CH_2Cl_2 in a flask, and mPEG-NPC (1.08 g, 0.5 mmol) dissolved in 20 mL of anhydrous CH_2Cl_2 was added dropwise over 30 min into the flask at 0 °C overnight under a dry nitrogen atmosphere. The mixture was diluted with 60 mL of CH_2Cl_2 and washed three times with 10 mL of saturated NaCl solution. The combined organic phase was dried over anhydrous Na_2SO_4 for 4 h, concentrated and precipitated into cold diethyl ether twice. The product was collected by filtration and dried under vacuum for 24 h to give mPEG₄₅-Hyd with a yield of 72%. ^1H NMR (400 MHz, CDCl_3 , 25 °C, ppm, Fig. S1(C)†): δ 3.38-3.40 (peak a, 3H), δ 3.44-3.84 (peak b, 180 H), δ 4.22-4.29 (peak c, 2H).

Synthesis of mPEG₄₅-Hyd-DOX. The mPEG₄₅-Hyd (0.12 g, 0.06 mmol) and DOX-HCl (51.3 mg, 0.09 mmol) were dissolved in 10 mL of anhydrous DMF, and the reaction was processed in the presence of one drop of TFA at 60 °C for 48 h. Afterward, the mixture was purified by dialysis (MWCO 1000) against a mixed solvent of methanol/Milli-Q water (v/v, from 2/1 to 1/1) for 48 h. The red powder mPEG₄₅-Hyd-DOX was finally obtained after lyophilization with a yield of 67%. ^1H NMR (400 MHz, CDCl_3 , 25 °C, ppm, Fig. S1(D)†): δ 1.28-1.30 (peak d, 3H), δ 5.35-5.42 (peak e, 2H), δ 7.59-8.56 (peaks f, g, h, 3H) attributed to the protons of aryl groups of DOX.

Rheological analysis of supramolecular hydrogels

To investigate the gelation kinetics of aqueous mPEG₄₅-Hyd-DOX/ α -CD system, time sweep tests were performed on a constant oscillatory frequency (1.0 rad s⁻¹) by a RS 6000 rheometer (Thermo Hakke) with parallel plate geometry (20 mm diameter, 0.1 mm gap) at 25 °C. In this case, all samples were placed on the plate immediately after the mixing and the measurement started after standing for 1 min. The viscoelastic parameters were measured as a function of time within the linear viscoelastic region previously determined by a strain scan. Frequency sweep tests were conducted with the help of the same instrument and the hydrogel sample was allowed to consolidate for 24 h before the analysis. The frequency applied to hydrogel sample increased from 0.1 to 100 rad s⁻¹. In addition, steady rate sweep tests were carried out to investigate the shear thinning property of the resultant hydrogels. In this case, the hydrogel samples were also allowed to consolidate for 24 h before the measurements.

In vitro loading and release of DOX

The DOX-loaded supramolecular hydrogel was prepared by an *in situ* forming method. Briefly, 45 mg of α -CD and 10 mg of mPEG₄₅-Hyd-DOX were individually dissolved in 0.3 and 0.2 mL of Milli-Q water, and the two solutions were mixed thoroughly by stirring for 60 s. Then the mixed solution was divided into 6 pieces in a 1 mL cuvette and stood for 24 h to yield the hydrogel. The cuvette was placed in a test tube with 20 mL of PB (pH 7.4 or pH 5.0) and incubated in a shaking water bath at 37 °C. At the desired time intervals, 5 mL of the released medium was withdrawn for fluorescence analysis and 5 mL of corresponding fresh buffer was added to keep a constant volume. The solution was measured by fluorescence spectroscopy with excitation at 480 nm and emission at 560 nm, and the slit width was set at 1 nm. All the loading and release experiments were carried out in dark.

Cell viability test

HeLa cells were purchased from the American Type Culture Collection. The cells were cultured in DMEM medium containing 10% heat-inactivated fetal bovine serum and 1% penicillin/streptomycin solution at 37 °C under a 5% CO_2 atmosphere and were used in their growth state. The culture media were replaced every three days.

The anticancer activity of the supramolecular hydrogel was evaluated by the methyl tetrazolium (MTT) assay using free DOX and mPEG₄₅-Hyd-DOX as the controls. A total of 30 mg of freeze-dried hydrogel sample (containing 1.5 mg DOX) was put into 3 mL of Milli-Q water in a 10 mL centrifuge tube, and then placed in a shaker incubator (37 °C) for two days. After that, the media were filtered with a 0.22 μm of sterile filter into a sterilized container and stored in a refrigerator at 4 °C before use. In addition, in order to investigate the anticancer activity of the released DOX from the hydrogels, HeLa cells were incubated with the released samples separately withdrawn from hydrogels at different time points in pH 5.0 or 7.4 PB solutions. HeLa cells were seeded onto a 96-well plate at a density of about 5×10^3 cells per well for 12 h. The sample solutions with different concentrations were then added to the wells and cultured for another 48 h. Afterwards, 25 μL of MTT stock solution (5 mg mL⁻¹ in PBS) were added to each well. After incubation for another 4 h, the DMEM medium was removed and the produced purple formazan was dissolved by adding 150 μL of DMSO. The optical density (OD) at 570 nm of each well was measured on a microplate reader (Bio-Rad 680). The absorbance values were normalized to the wells in which cells were not treated with samples. The cell viability was calculated by the equation: $\text{OD}_{\text{sample}}/\text{OD}_{\text{control}} \times 100\%$, in which $\text{OD}_{\text{sample}}$ and $\text{OD}_{\text{control}}$ are the absorbance values of the testing well (in the presence of samples) and the control well (in the absence of samples), respectively. Data are presented as average values with standard deviations.

Results and discussion

Synthesis and characterization of polymeric prodrug

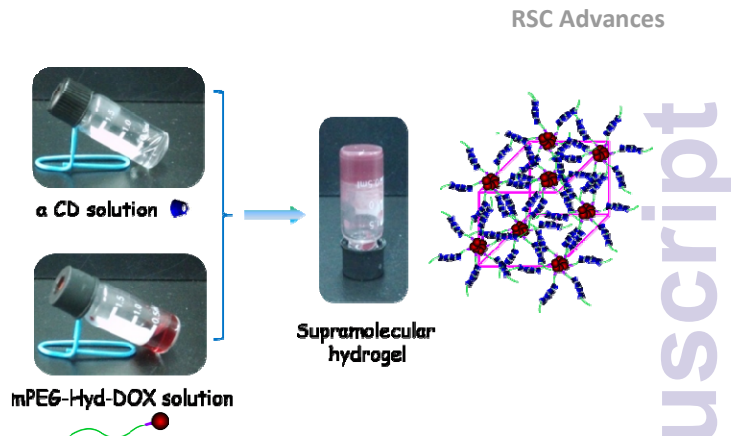
As shown in Scheme 1, the pH-sensitive prodrug mPEG₄₅-Hyd-DOX was synthesized *via* the following three steps: (1)

ARTICLE

synthesis of mPEG₄₅-NPC; (ii) synthesis of mPEG₄₅-Hyd; and (iii) preparation of mPEG₄₅-Hyd-DOX. Firstly, the hydroxyl group of mPEG₄₅-OH was activated with 4-nitrophenyl chloroformate to generate mPEG₄₅-NPC. In the second step, the mPEG₄₅-NPC was further reacted with hydrazine monohydrate to give mPEG₄₅-Hyd. The resultant products in each step were characterized by ¹H NMR as shown in Fig. S1†. The peaks at δ 3.44–3.84 and δ 3.39 ppm in Fig. S1(A)† were attributed to the protons of the main chain of PEG and the terminal methyl group of PEG, respectively. After modification, comparing with mPEG₄₅-OH, the ¹H NMR spectrum of mPEG₄₅-NPC in Fig. S1(B)† exhibits new peaks at δ 4.45 ppm (peak c), δ 7.40 ppm (peak d) and δ 8.30 ppm (peak e), demonstrating the successful modification. In addition, the integral value ratio of peaks a, c, d and e (1.56: 1.05: 0.96: 1.00) implies that most of the hydroxyl group of mPEG₄₅-OH was activated. From the ¹H NMR spectrum of mPEG₄₅-Hyd shown in Fig. S1(C)†, the disappearance of the signals at δ 7.40 and 8.30 ppm, as well as the chemical shift from the original signal at δ 4.45 ppm in Fig. S1(B)† to δ 4.26 ppm confirmed the successful synthesis of mPEG₄₅-Hyd. FT-IR measurements were also used to characterize the polymers and the results are shown in Fig. S2†. Finally, mPEG₄₅-Hyd-DOX was synthesized by the reaction of the hydrazine bond of mPEG₄₅-Hyd with the carbonyl group of DOX, and the obtained mPEG₄₅-Hyd-DOX was confirmed by ¹H NMR and HPLC. The successful conjugation of mPEG₄₅-Hyd with DOX was proven by the peaks at δ 7.56–8.59 and 1.27 ppm in the ¹H NMR spectrum of mPEG₄₅-Hyd-DOX, as shown in Fig. S1(D)†. Meanwhile, HPLC showed that the retention time of free DOX was 1.11 min, while that of PEG₄₅-Hyd-DOX was 4.02 min under the same condition, as shown in Fig. S3(A)† and Fig. S3(B)†. On the other hand, the hydrazone linker was hydrolyzed and gradually cleaved at low pH condition. Incubation of PEG₄₅-Hyd-DOX at 1 M HCl for 1 h led to the complete degradation of the hydrazone bonds, resulting in the elution peaks in Fig. S3(C)†, corresponding to that of free DOX. The DOX content of the polymeric prodrug was about 29 wt%, according to the fluorescence spectroscopy with excitation at 480 nm and emission at 560 nm.

Preparation of supramolecular hydrogel

Supramolecular hydrogel was prepared by directly mixing the α-CD solution with prodrug solution as shown in Scheme 2. The polymeric prodrug mPEG₄₅-Hyd-DOX could be dissolved in water and formed supramolecular hydrogel when α-CD was introduced. This gelation procedure could occur under mild conditions without high temperature and the use of chemical cross-linker, which was only dependent on the amounts of mPEG₄₅-Hyd-DOX and α-CD. The formation of supramolecular hydrogel was based on the host-guest inclusion complexation between α-CD and PEG chain.³ It is well-known that α-CD could form crystalline inclusion complexes with low-molecular-weight PEG in aqueous solution. Here the inclusion complexes formed by α-CD and PEG chain of mPEG₄₅-Hyd-DOX may be thought to aggregate into the microcrystals, which acted as



Scheme 2. The digital photographs of the sol-gel transition of mPEG₄₅-Hyd-DOX prodrug and α-CD solutions.

physical crosslinkers and then induced the formation of supramolecular hydrogel networks.

Time-sweep rheological analyses were performed to monitor hydrogel network evolution and evaluate the viscoelastic behavior. Three fixed concentrations of mPEG₄₅-Hyd-DOX aqueous solutions (1.0, 2.0 and 3.0 wt%) and three concentrations of α-CD aqueous solutions (7.0, 9.0 and 11.0 wt%) were used for the study. To investigate the effects of amounts of mPEG₄₅-Hyd-DOX and α-CD on the gelation, time-sweep measurements were carried out, in which the storage modulus (G') and loss modulus (G'') were monitored as a function of time. As shown in Fig. 1 and Fig. 2, during the gelation procedure, both moduli increased and the G' values became larger than the G'' values, indicating that the systems became more elastic and formed a series of physically cross-linked networks. It is well known that a crossover point (G' = G'') of G' and G'' curves was detected for a gelation process (from G' < G'' to G' > G''). The corresponding time of the crossover from a viscous behavior to an elastic response could be regarded as the gelation time. In this work, all the crossover points were observed and the gelation time was very short, indicating that this class of supramolecular hydrogel possesses fast gelation. From Fig. 1(A)~(C), the gelation time was found to decrease with the increase of α-CD amounts. When the concentration of α-CD increased gradually from 7.0, 9.0 to 11.0 wt%, namely, 35, 45 and 55 mg of α-CD alone in 0.5 mL of H₂O, while the amount of mPEG₄₅-Hyd-DOX was fixed at 10 mg in 0.5 mL of H₂O, the gelation time for the three systems decreased respectively from 167, 108 and finally to 39 s. In contrast, when the α-CD amount was fixed at 45 mg in 0.5 mL of H₂O, while the amount of mPEG₄₅-Hyd-DOX was gradually increased from 1.0, 2.0 to 3.0 wt%, that is, 5, 10 and 15 mg alone in 0.5 mL of H₂O, the corresponding gelation time decreased from 190, 108 to 101 s, respectively, as shown in Fig. 2(A)~(C). These results indicate that the enhanced amounts of α-CD and mPEG₄₅-Hyd-DOX prodrug would accelerate the gelation time, and the inclusion complexation between α-CD and mPEG₄₅-Hyd-DOX induced the formation of supramolecular hydrogel, which could fix the anticancer drug DOX into the networks.

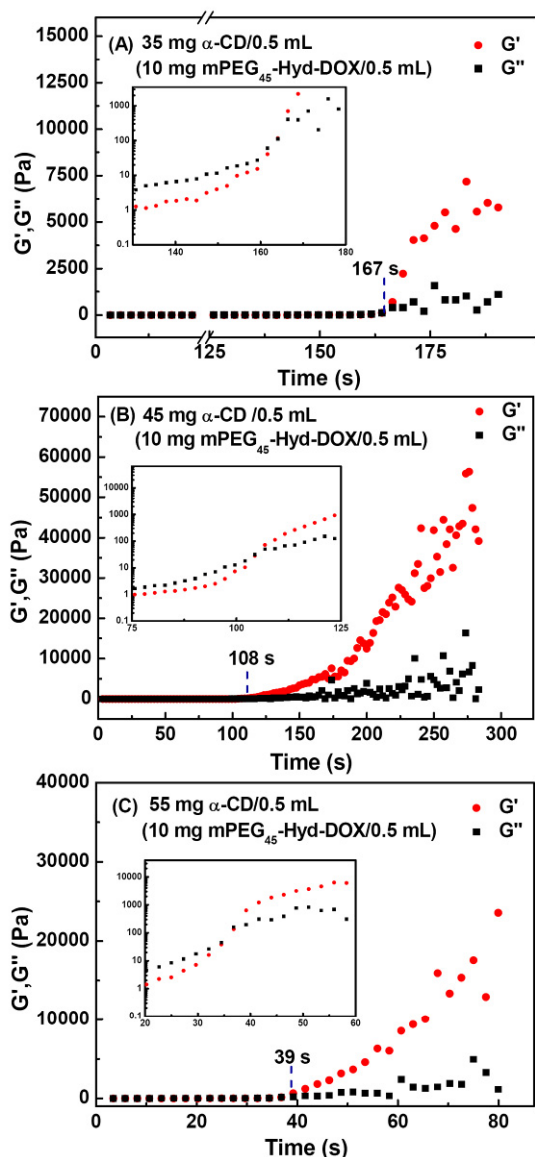


Fig. 1. Effects of the amounts of α -CD on the gelation time of the gelled mPEG₄₅-Hyd-DOX/ α -CD systems. The insets show the representative magnification of the crossover of the storage modulus (G') and loss modulus (G'') curves. Test conditions: frequency, 1.0 rad s⁻¹; strain, 1%; temperature, 25 °C.

For the resultant supramolecular hydrogels, their storage modulus (G') and shear-dependent viscosity (η) were also investigated with respect to the effects of the amounts of α -CD and mPEG₄₅-Hyd-DOX. The G' values increased with the increase of α -CD or mPEG₄₅-Hyd-DOX amount at a fixed frequency or shear rate, as shown in Fig. 3. At a frequency of 1.0 rad s⁻¹, for example, the G' value increased from 10.4 to 31.6 kPa when the amount of α -CD increased from 7.0 to 9.0 wt%; while the G' value increased from 6.8 to 20.9 kPa when the amount of mPEG₄₅-Hyd-DOX increased from 1.0 to 3.0 wt%. In addition, all the G' values showed a weak dependence on frequency, which confirmed that the hydrogels were well cross-linked with insignificant sol fraction. It is widely reported that shear-thinning property is required and important for the injectable drug delivery systems, which have recently drawn

great attentions due to the minimization of surgical implantation.⁴⁶ Fig. 4 shows the steady shear viscosity as a function of shear rate for the *in situ* forming supramolecular hydrogels under various amounts of mPEG₄₅-Hyd-DOX and α -CD. One can find that the viscosity of the hydrogels decreased greatly when it was sheared, which was independent of the amounts of mPEG₄₅-Hyd-DOX or α -CD. This property indicates that the supramolecular hydrogels may be injected into body through a hypodermic needle.

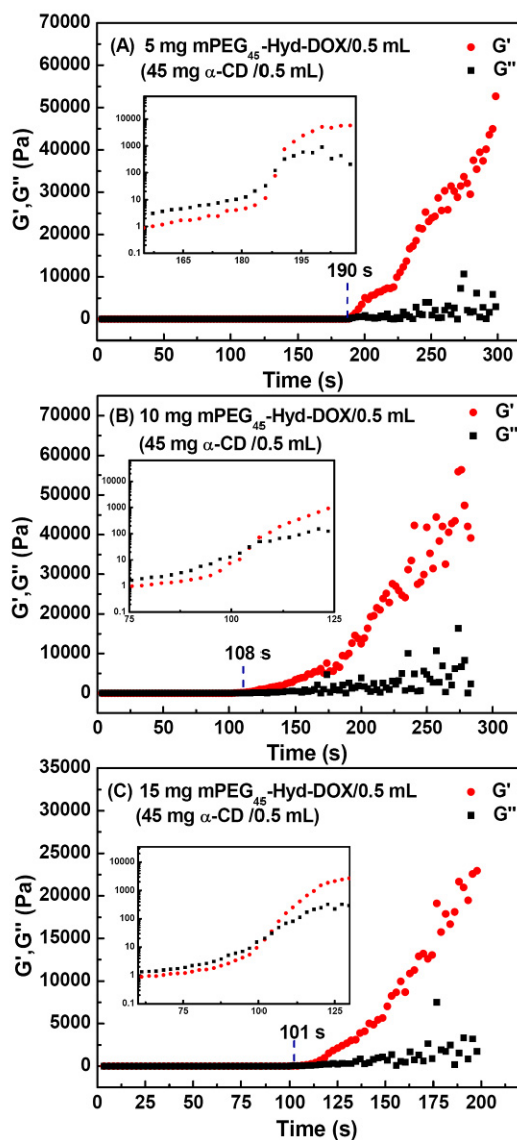


Fig. 2. Effects of the amounts of mPEG₄₅-Hyd-DOX on the gelation time of the gelled mPEG₄₅-Hyd-DOX/ α -CD systems. The insets show the representative magnification of the crossover of the storage modulus (G') and loss modulus (G'') curves. Test conditions: frequency, 1.0 rad s⁻¹; strain, 1%; temperature, 25 °C.

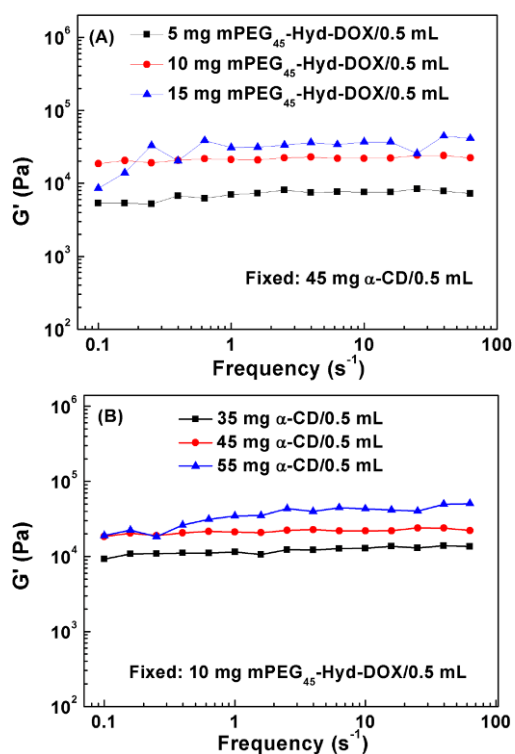


Fig. 3. Effects of the amounts of mPEG₄₅-Hyd-DOX and α -CD on the elastic modulus (G') of the gelled mPEG₄₅-Hyd-DOX/ α -CD systems. Test conditions: strain, 1%; temperature, 25 °C.

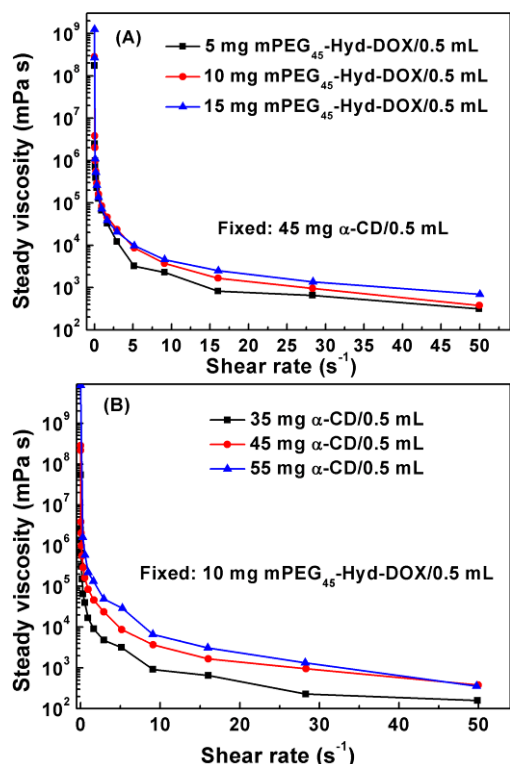


Fig. 4. Effects of the amounts of (A) α -CD and (B) mPEG₄₅-Hyd-DOX on the shear-dependent viscosity of the gelled mPEG₄₅-Hyd-DOX/ α -CD systems. Test conditions: strain, 1%; temperature, 25 °C.

Properties of freeze-dried hydrogels

In biomedical applications, such as tissue engineering and drug delivery, the morphological structure of hydrogels is an important factor to be taken into consideration. The morphology of the hydrogels was analyzed by the scanning electron microscopy (SEM) because high water content of the swollen hydrogels will likely lead to highly macroporous scaffolds upon lyophilization. As shown in Fig. 5(A)~(D), the freeze-dried hydrogels clearly exhibited the presence of the typical porous structures. These porous structures are indispensable to allow for tissue growth and diffusion of drugs and nutrients. Therefore, a higher percentage of pore fractions and smaller pore size were obtained by increasing the α -CD amount from 35, 45 to 55 mg, which might be due to the increase of network density.

To confirm the inclusion complexation, we measured XRD patterns of the freeze-dried hydrogel formed from 10 mg of mPEG₄₅-Hyd-DOX and 45 mg of α -CD solutions, α -CD and mPEG₄₅-Hyd-DOX, respectively. As shown in Fig. 6, the freeze-dried hydrogel was observed to have two characteristic diffraction peaks at $2\theta = 19.73^\circ$ and 22.38° , which were not observed in the separate patterns of mPEG₄₅-Hyd-DOX or α -CD. α -CD was characteristic of multiple diffraction peaks corresponding to its crystalline formation, and mPEG₄₅-Hyd-DOX showed two obvious diffraction peaks at $2\theta = 19.20^\circ$ and 23.39° . After the PEG chain was threaded into the α -CD inner core, the different crystallines would be formed. Two new peaks in freeze-dried hydrogel could represent the channel-type crystalline structure of mPEG₄₅-Hyd-DOX/ α -CD complex.⁵⁸

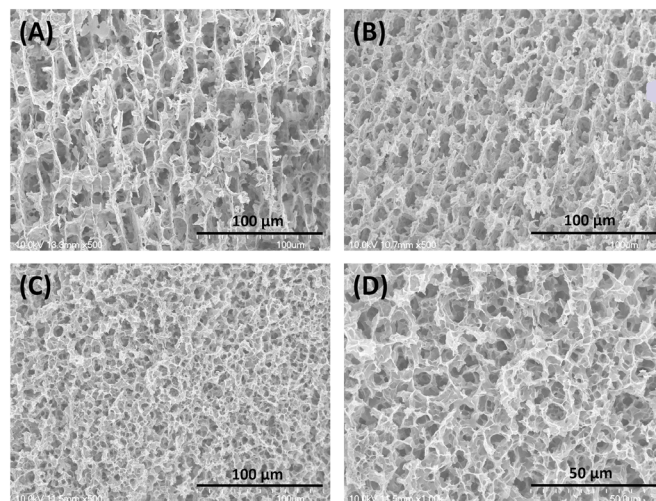


Fig. 5. SEM images of the freeze-dried hydrogel: (A) 10 mg mPEG₄₅-Hyd-DOX and 35 mg α -CD/0.5 mL H₂O, scale bar = 100 μ m; (B) 10 mg mPEG₄₅-Hyd-DOX and 45 mg α -CD/0.5 mL H₂O, scale bar = 100 μ m; (C) and (D) 10 mg mPEG₄₅-Hyd-DOX and 55 mg α -CD/0.5 mL H₂O with scale bars of 100 μ m and 50 μ m, respectively.

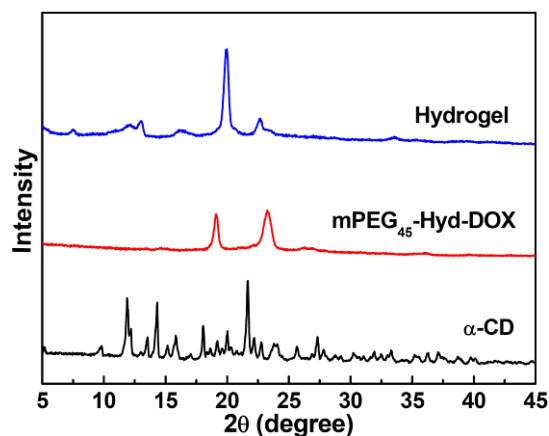


Fig. 6. XRD patterns of α -CD, mPEG₄₅-Hyd-DOX and the freeze-dried hydrogel from 10 mg mPEG₄₅-Hyd-DOX and 45mg α -CD/0.5 mL H₂O.

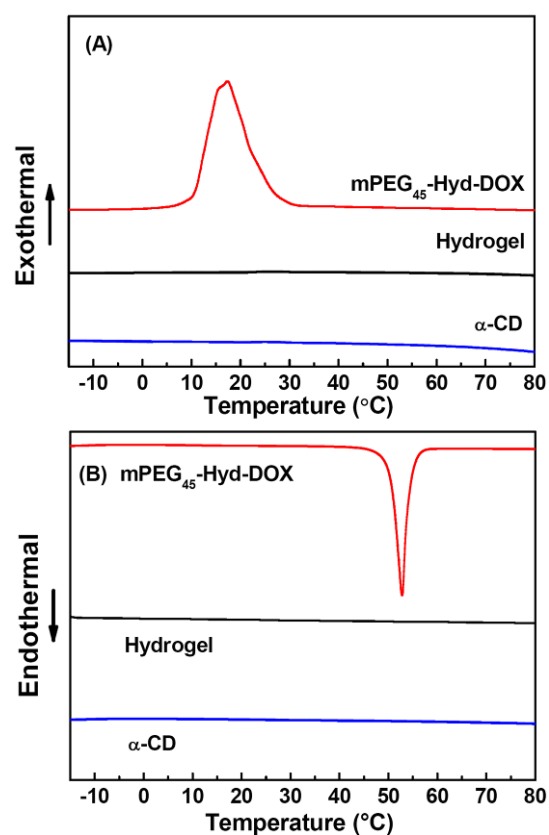


Fig. 7. DSC curves of (A) the cooling run and (B) the second heating run of α -CD, mPEG₄₅-Hyd-DOX and the freeze-dried hydrogel.

When PEG chain threads into the inner core of α -CD, it will bring different thermal properties to the inclusion complex. From Fig. 7(A), a distinct exothermic peak at 17.2 °C, that is the crystallization temperature (T_c), was observed for mPEG₄₅-Hyd-DOX in the cooling run, corresponding to the crystallization temperature of PEG chain crystalline. However, the freeze-dried hydrogel did not show any obvious peak, which was similar with that of α -CD and implied that PEG chain was included into the inner core of α -CD so as to impede the crystallization of PEG chain. As the same in Fig. 7(B), a strong

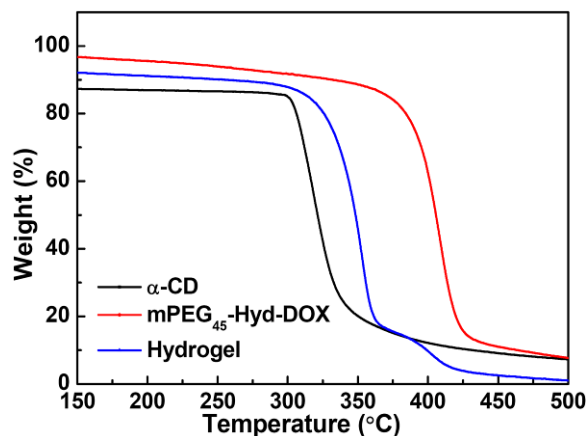


Fig. 8. TGA curves of α -CD, mPEG₄₅-Hyd-DOX and the freeze-dried hydrogel from 10 mg of mPEG₄₅-Hyd-DOX and 45 mg of α -CD/0.5 mL H₂O.

melting peak was detected for mPEG₄₅-Hyd-DOX at around 377 °C in the second heating run, resulting from the melting of PEG chain. However, there was no observed melting peak corresponding to the melting of mPEG, because the PEG chain was hid into the inner core of α -CD with the disappearance of any melting behavior. The similar phenomenon has also been reported previously.²⁹ In addition, TGA analysis was also performed to study the supramolecular hydrogel. As shown in Fig. 8, TGA curves revealed that α -CD had a higher decomposition temperature ($T_d = 315$ °C) after threading onto PEG chain than α -CD ($T_d = 300$ °C), implying that the PEG chain included inside the α -CD molecules improve the thermal stability of the α -CD. Meanwhile, the left mPEG₄₅-Hyd-DOX in the freeze-dried hydrogel showed the same decomposition temperature at 377 °C like that of mPEG₄₅-Hyd-DOX when the α -CD was mostly decomposed.

In vitro drug release and cytotoxicity

To investigate the effect of pH values on drug release, the *in vitro* release experiments of DOX were performed in two different buffer solutions of pH 5.0 and 7.4, respectively. The supramolecular hydrogels were formed by mixing 10 mg of mPEG₄₅-Hyd-DOX and 45 mg of α -CD in pH 7.4 and pH 5.0 conditions at 37 °C. Fig. 9 shows the cumulative release curves of DOX. In the case of pH 5.0, there was a controlled and sustained release behavior without initial burst release. Obviously, the DOX was released much faster at pH 5.0 than that at pH 7.4, indicating that the pH-sensitive hydrazone linker was cleaved faster in the acidic environment, which could accelerate the disintegration of the supramolecular hydrogel and release the native DOX. It is anticipated that other therapeutic agents could be loaded into the hydrogel matrix by simple premixing and released at the tumor environment.

Finally, the *in vitro* cytotoxicity of free DOX, mPEG₄₅-Hyd-DOX prodrug and the supramolecular hydrogel formed from 10 mg of mPEG₄₅-Hyd-DOX and 45 mg of α -CD/0.5 mL of H₂O were tested by MTT assay against HeLa cells. All the samples were kept at an equivalent DOX concentration. Fig. 10 shows

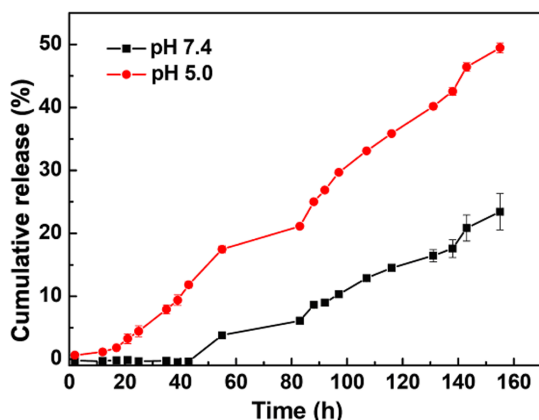


Fig. 9. *In vitro* release curves of the supramolecular hydrogel in pH 5.0 and pH 7.4 PB solutions, respectively.

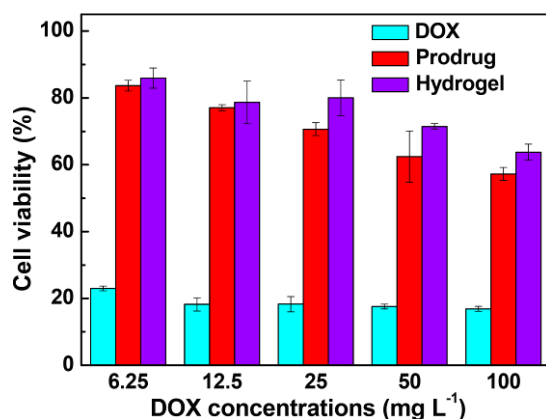


Fig. 10. Cell viabilities of HeLa cells incubated with free DOX, mPEG₄₅-Hyd-DOX prodrug and hydrogel with different DOX concentrations for 48 h.

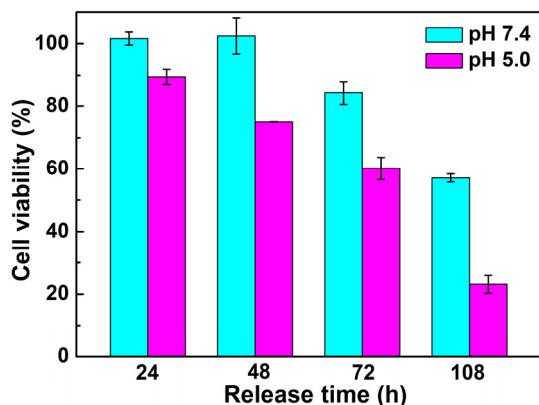


Fig. 11. Cell viability of HeLa cells incubated with the solutions released at different time points in pH 7.4 and pH 5.0, respectively. All of the samples were incubated with HeLa cells for 48 h.

that the cell viability of HeLa cells incubated with free DOX was extremely low, but for the mPEG₄₅-Hyd-DOX prodrug with equal DOX concentration, the cell viability was still 60% after 48 h at a high concentration of 100 mg L⁻¹. PEG does not only improve the water solubility of free DOX, but also decrease its cytotoxicity. Similar results about the polymeric prodrugs have also been reported elsewhere.^{42,54} Interestingly, the cell viability of hydrogel was higher than that of mPEG₄₅-Hyd-DOX

prodrug at the equal concentrations, which could be attributed to the favorable biocompatibility of α -CD. In addition, we have investigated the anticancer activity of the released DOX separately withdrawn from the hydrogels at different time points in pH 5.0 or 7.4 PB solutions. As shown in Fig. 11, the samples released at first 48 h showed minimal cytotoxicity in pH 7.4 PB solution, while the samples released at the same time in pH 5.0 PB solution showed much higher cytotoxicity. In the mean time, both of the released samples showed increased cytotoxicities with the prolongation of release time in 7.4 and 5.0 PB solutions.

Conclusions

A series of novel supramolecular hydrogels have been prepared *via* host-guest inclusion complexation between a polymeric prodrug mPEG₄₅-Hyd-DOX and α -CD. Because the hydrogels contain the acid-cleavable hydrazone bonds, the hydrogels were easy degraded in the tumor cell environment and released the fixed anticancer drug DOX. Meanwhile, the hydrogels possessed the characteristics of supramolecular hydrogels, especially *in situ* formation, porous structure and shear-thinning properties. In addition, the resultant supramolecular hydrogels had the adjustable gelation time and mechanical strength, depending on the amounts of mPEG₄₅-Hyd-DOX prodrug and α -CD. The excess amounts of both prodrug and α -CD could accelerate the gelation process. This study presents a hydrogel carrier based on pH-sensitive polymeric prodrugs to deliver poorly water-soluble drugs, which would find potentials in injectable drug delivery systems.

Acknowledgements

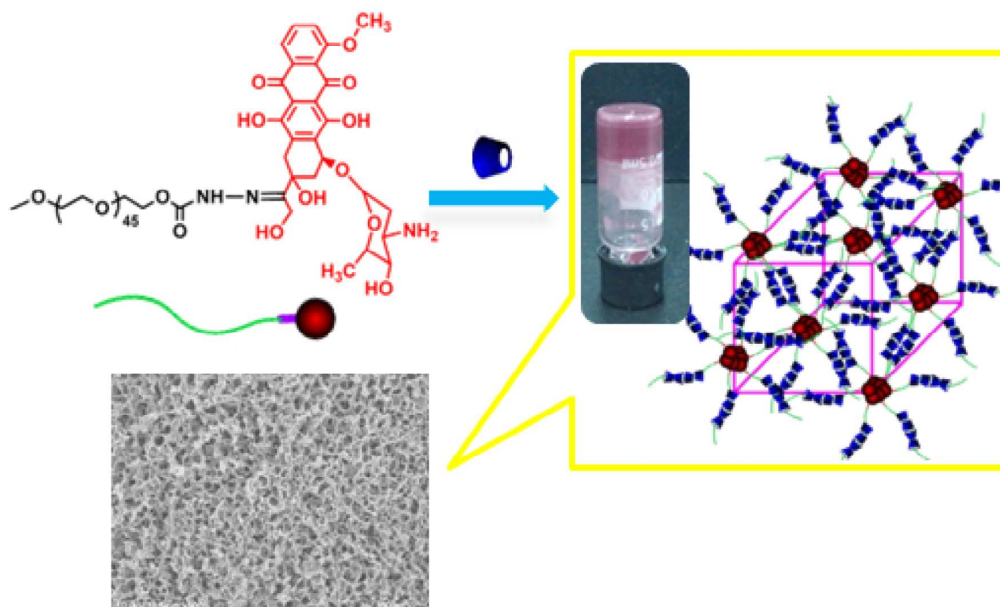
The authors gratefully acknowledge financial supports from the National Natural Science Foundation of China (21374066 and 21074078), Suzhou Science and Technology Program for Industrial Application Foundation (SYG201429), Natural Science Foundation of Jiangsu Province (BK20130286), a Project Funded by the Priority Academic Program Development (PAPD) of Jiangsu Higher Education Institutions, and Soochow-Waterloo University Joint Project for Nanotechnology from Suzhou Industrial Park. We are also thankful to Professor Jian Liu (FUNSOM, Soochow University) for his kind help in the cell-related test.

References

1. N. M. Sangeetha and U. Maitra, *Chem. Soc. Rev.*, 2005, **34**, 821-836.
2. X. Ma and Y. L. Zhao, *Chem. Rev.*, 2015, doi: 10.1021/cr500392w.
3. J. Li, Z. P. Ni and K. W. Leong, *J. Biomed. Mater. Res. A*, 2007, **65A**, 196-202.
4. J. Li, *NPG Asia Mater.* 2010, **2**, 112-118.
5. H. Zou, W. Guo and W. Z. Yuan, *J. Mater. Chem. B*, 2013, **1**, 6235-6244.
6. R. Mateen and T. Hoare, *J. Mater. Chem. B*, 2014, **2**, 5157-5167.

- 7 D. Ma, K. Tu and L. M. Zhang, *Biomacromolecules*, 2010, **11**, 2204-2212.
- 8 H. Hyun, Y. H. Kim, I. B. Song, J. W. Lee, M. S. Kim, G. Khang, K. Park and H. B. Lee, *Biomacromolecules*, 2007, **8**, 1093-1100.
- 9 J. Liand X.J. Loh, *Adv. Drug Deliver. Rev.*, 2008, **60**, 1000-1017.
- 10 D. Q. Wu, T. Wang, B. Lu, X. D. Xu, S. X. Cheng, X. J. Jiang, X. Z. Zhang and R. X. Zhuo, *Langmuir*, 2008, **24**, 10306-10312.
- 11 K. Y. Lee and D. J. Mooney, *Chem. Rev.*, 2001, **101**, 1869-1879.
- 12 N. P. Rhodes, *Biomaterials*, 2007, **28**, 5131-5136.
- 13 L. Yu, G. T. Chang, H. Zhang and J. D. Ding, *Int. J. Pharm.*, 2008, **348**, 95-106.
- 14 B. G. Xing, C. W. Yu, K. H. Chow, P. L. Ho, D. G. Fu and B. Xu, *J. Am. Chem. Soc.*, 2002, **124**, 14846-14847.
- 15 F. Yuen and K. C. Tam, *Soft Matter*, 2010, **6**, 4613-4630.
- 16 D. Ma, H. B. Zhang, K. Tu and L. M. Zhang, *Soft Matter*, 2012, **8**, 3665-3672.
- 17 Y. Guan, H. B. Zhao, L. X. Yu, S. C. Chen and Y. Z. Wang, *RSC Adv.*, 2014, **4**, 4955-4959.
- 18 J. Yu, W. Ha, J. Chen and Y. P. Shi, *RSC Adv.*, 2014, **4**, 58982-58989.
- 19 J. N. Hunt, K. E. Feldman, N. A. Lynd, J. Deek, L. M. Campos, J. M. Spruelli, B. M. Hernandez, E. J. Kramer and C. J. Hawker, *Adv. Mater.*, 2011, **23**, 2327-2331.
- 20 M. Lemmers, J. Sprakel, I. K. Voets, J. van der Gucht and M. A. Cohen Stuart, *Angew. Chem., Int. Ed.*, 2010, **49**, 708-711.
- 21 Y. Xiao, J. L. He, Y. F. Tao, M. Z. Zhang, J. Hu, and P. H. Ni, *Acta Polym. Sin.*, 2014, **1**, 122-130.
- 22 S. J. Buwalda, P. J. Dijkstra and J. Feijen, *J. Polym. Sci. Part A: Polym. Chem.*, 2012, **50**, 1783-1791.
- 23 Y. Zhang, H. W. Gu, Z. M. Yang and B. Xu, *J. Am. Chem. Soc.*, 2003, **125**, 13680-13681.
- 24 E. A. Appel, J. del Barrio, X. J. Loh and O. A. Scherman, *Chem. Soc. Rev.*, 2012, **41**, 6195-6214.
- 25 J. Li, X. Li, Z. H. Zhou, X. P. Ni and K. W. Leong, *Macromolecules*, 2001, **34**, 7236-7237.
- 26 G. S. Chen and M. Jiang, *Chem. Soc. Rev.*, 2011, **40**, 2254-2266.
- 27 A. Hashidzume and Akira Harada, *Poly. Chem.*, 2011, **2**, 2146-2154.
- 28 A. Harada and Y. Takashima, *Chem. Rec.*, 2013, **13**, 420-431.
- 29 Z. C. Tian, C. Chen and H. R. Allcock, *Macromolecules*, 2013, **46**, 2715-2724.
- 30 M. Nakahata, Y. Takashima, H. Yamaguchi and A. Harada, *Nat. Commun.*, 2011, **2**, 511-516.
- 31 X. J. Liao, G. S. Chen, X. X. Liu, W. X. Chen, F. Chen and M. Jiang, *Angew. Chem. Int. Ed.*, 2010, **49**, 4409-4413.
- 32 K. Cho, X. Wang, S. M. Nie, Z. Chen and D. M. Shin, *Clin. Cancer Res.*, 2008, **14**, 1310-1316.
- 33 K. Kataoka, A. Harada and Y. Nagasaki, *Adv. Drug Deliv. Rev.*, 2001, **47**, 113-131.
- 34 H. R. Wang, J. L. He, M. Z. Zhang, Y. F. Tao, F. Li, K. C. Tam and P. H. Ni, *J. Mater. Chem. B*, 2013, **1**, 6596-6607.
- 35 Y. Zhang, J. L. He, D. L. Cao, M. Z. Zhang and P. H. Ni, *Polym. Chem.*, 2014, **5**, 5124-5138.
- 36 D. L. Wang, T. Y. Zhao, X. Y. Zhu, D. Y. Yan and W.X. Wang, *Chem. Soc. Rev.*, 2015, doi: 10.1039/c4cs00229f.
- 37 M. Calderón, M. A. Quadir, S. K. Sharma and R. Haag, *Adv. Mater.*, 2010, **22**, 190-218.
- 38 C. C. Lee, E. R. Gillies, M. E. Fox, S. J. Guillaudeu, J. M. Fréchet, E. E. Dy and F. C. Szoka, *Proc. Natl. Acad. Sci. U. S. A.*, 2006, **103**, 16649-16654.
- 39 T. M. Allen and P. R. Cullis, *Science*, 2004, **303**, 1818-1822.
- 40 W. Chen, F. H. Meng, R. Cheng and Z. Y. Zhong, *J. Controlled Release*, 2010, **142**, 40-46.
- 41 P. F. Gou, W. W. Liu, W. W. Mao, J. B. Tang, Y. Q. Shen and M. H. Sui, *J. Mater. Chem. B*, 2013, **1**, 284-292.
- 42 G. Y. Zhang, M. Z. Zhang, J. L. He and P. H. Ni, *Polym. Chem.*, 2013, **4**, 4515-4525.
- 43 Y. D. Gu, Y. N. Zhong, F. H. Meng, R. Cheng, C. Deng and Z. Y. Zhong, *Biomacromolecules*, 2013, **14**, 2772-2780.
- 44 M. J. Zou, H. Okamoto, G. Cheng, X. H. Hao, J. Sun, F. D. Cui and K. Danjo, *Eur. J. Pharm. Biopharm.*, 2005, **59**, 155-160.
- 45 V. Delplace, P. Couvreur and J. Nicolas, *Polym. Chem.*, 2014, **5**, 1529-1544.
- 46 D. Ma and L. M. Zhang, *Biomacromolecules*, 2011, **12**, 3124-3130.
- 47 W. Ha, J. Yu, X. Y. Song, Z. J. Zhang, Y. Q. Liu and Y. P. Shi, *J. Mater. Chem. B*, 2013, **1**, 5532-5538.
- 48 S. M. Swain, F. S. Whaley, M. C. Gerber, M. S. Ewer, J. R. Bianchini and R. A. Gams, *J. Clin. Oncol.*, 1997, **15**, 1333-1340.
- 49 R. P. A'Hern and M. E. Gore, *J. Clin. Oncol.*, 1995, **13**, 726-732.
- 50 A. M. Murad, F. F. Santiago, A. Petroianu, P. R. S. Rocha, M. A. G. Rodrigues and M. Rausch, *Cancer*, 1993, **72**, 37-41.
- 51 C. Carvalho, R. X. Santos, S. Cardoso, S. Correia, P. J. Oliveira, M. S. Santos and P. I. Moreira, *Curr. Med. Chem.*, 2009, **16**, 3267-3285.
- 52 X. L. Hu, S. Liu, Y. B. Huang, X. S. Chen and X. B. Jing, *Biomacromolecules*, 2010, **11**, 2094-2102.
- 53 J. W. Cui, Y. Yan, Y. J. Wang and F. Caruso, *Adv. Funct. Mater.*, 2012, **22**, 4718-4723.
- 54 X. J. Chen, S. S. Parelkar, E. Henchey, S. Schneider and T. Emrick, *Bioconjugate Chem.*, 2012, **23**, 1753-1763.
- 55 X. Guo, C. L. Shi, J. Wang, S. B. Di and S. B. Zhou, *Biomaterials*, 2013, **34**, 4544-4554.
- 56 E. S. Lee, Z. G. Gao and Y. H. Bae, *J. Controlled Release*, 2008, **132**, 164-170.
- 57 Y. Huang, Z. H. Tang, X. F. Zhang, H. Y. Yu, H. Sun, X. Pang and X. S. Chen, *Biomacromolecules*, 2013, **14**, 2023-2032.
- 58 W. Ha, J. Yu, X. Y. Song, J. Chen and Y. P. Shi, *ACS Appl. Mater. Interfaces*, 2014, **6**, 10623-10630.

Graphical Abstract



Fabrication of *in situ* forming and acid-labile prodrug-based supramolecular hydrogels with adjustable gelation time for injectable drug delivery carriers.